16

High-gain Millimeter-wave Planar Array Antennas with Traveling-wave Excitation

Kunio Sakakibara
Nagoya Institute of Technology
Japan

1. Introduction

High-gain and large-aperture antennas with fixed beams are required to achieve high S/N ratio for point-to-point high-speed data-communication systems in the millimeter-wave band. Furthermore, beam-scanning antennas are attractive to cover wide angle with high gain for applications of high-speed data-communication systems and high-resolution sensing systems. High-gain pencil-beam antennas are used for mechanical beam-scanning antennas. Although high antenna efficiency can be obtained by using dielectric lens antennas or reflector antennas (Kitamori et al., 2000, Menzel et al., 2002), it is difficult to realize very thin planar structure because they essentially need focal spatial length. By using printed antennas such as microstrip antennas, the RF module with integrated antennas can be quite low profile and low cost. Array antennas possess a high design flexibility of radiation pattern. However, microstrip array antennas are not suitable for high-gain applications because large feeding-loss of microstrip line is a significant problem when the size of the antenna aperture is large. They are applied to digital beam forming (DBF) systems since they consist of several sub-arrays, each of which has small aperture and requires relatively lower gain (Tokoro, 1996, Asano, 2000, Iizuka et al., 2003).
Slotted waveguide planar array antennas are free from feeding loss and can be applied to both high-gain antennas and relatively lower-gain antennas for sub-arrays in beam-scanning antennas. Waveguide antennas are more effective especially in high-gain applications than low-gain since a waveguide has the advantage of both low feeding loss and compact size in the millimeter-wave band even though the size of the aperture is large (Sakakibara et al., 1996). However, the production cost of waveguide antennas is generally very high because they usually consist of metal block with complicated three-dimensional structures. In order to reduce the production cost without losing a high efficiency capability, we propose a novel simple structure for slotted waveguide planar antennas, which is suitable to be manufactured by metal injection molding (Sakakibara et al., 2001).
We have developed two types of planar antenna; microstrip antenna and waveguide antenna. It is difficult to apply either of them to all the millimeter-wave applications with different specifications since advantages of the antennas are completely different. However, most applications can be covered by both microstrip antennas and waveguide antennas. Microstrip antennas are widely used for relatively lower-gain applications of short-range wireless-systems and sub-arrays in DBF systems, not for high-gain applications. Waveguide antennas are suitable for high-gain applications over 30 dBi.

Source: Radar Technology, Book edited by: Dr. Guy Kouemou,
ISBN 978-953-307-029-2, pp. 410, December 2009, INTECH, Croatia, downloaded from SCIYO.COM

With regard to the microstrip antennas, comb-line antennas are developed in the millimeter-wave band. In the comb-line antenna, since radiating array-element is directly attached to the feeding line, feeding loss could be quite small in comparison with other ordinary patch array antennas connected via microstrip branch from feeding lines. The branch of the comb-line antenna is no longer feeding circuit but radiating element itself. Radiation from the discontinuity at the connection of the radiating element joins to the main radiation from the element. Consequently, equivalent circuit model can not be used in the design any more. Electromagnetic simulator must be used to estimate the amplitude and phase of radiation from the elements accurately. Traveling-wave excitation is assumed in the design of comb-line antennas. Reflection waves from the elements in the feeding line degrade the performance of the antenna. When all the radiating elements are excited in phase for broadside beam, reflection waves are also in-phase and return loss grows at the feeding point. Furthermore, reflection waves from elements re-radiate from other elements. Radiation pattern also degrades since it is not taken into account in the traveling-wave design. Therefore, reflection-canceling slit structure is proposed to reduce reflection from the radiating element. Feasibility of the proposed structure is confirmed in the experiment (Hayashi et al, 2008).

On the other hand in the design of conventional shunt and series slotted waveguide array antennas for vertical and horizontal polarization, radiation slots are spaced by approximately a half guided wavelength for in-phase excitation. Interleave offset and orientation from waveguide center axis are necessary to direct the main beam toward the broadside direction (Volakis, 2007). Since the spacing is less than a wavelength in free space, grating lobes do not appear in any directions. For bidirectional communication systems in general, two orthogonal polarizations are used to avoid interference between the two signals. In the case of automotive radar systems, 45-degrees diagonal polarization is used so that the antenna does not receive the signals transmitted from the cars running toward the opposite direction (Fujimura 1995). However, in the design of the slotted waveguide array antenna with arbitrarily linear polarization such as 45-degrees diagonal polarization for the automotive radar systems, slot spacing is one guided wavelength which is larger than a wavelength in free space. All the slots are located at the waveguide center with an identical orientation in parallel unlike conventional shunt and series slotted waveguide array. Consequently, grating lobes appear in the radiation pattern. Antenna gain is degraded significantly and ghost image could be detected in the radar system toward the grating-lobe direction. In order to suppress the grating lobes, dielectric material is usually filled in the waveguide (Sakakibara et al. 1994, Park et al. 2005). However, it would cause higher cost and gain degradation due to dielectric loss in the millimeter-wave band.

We have proposed a narrow-wall slotted hollow waveguide planar antenna for arbitrarily linear polarization (Yamamoto et al., 2004). Here, we developed two different slotted waveguide array antennas with 45-degrees diagonal linear polarization. One is quite high gain (over 30 dBi) two-dimensional planar array antenna (Mizutani et al. 2007) and the other one is a relatively lower gain (around 20 dBi) antenna which can be used for a sub-array in beam-scanning antennas (Sakakibara et al. 2008). Microstrip comb-line antenna is also developed for lower-gain applications of the sub-array. Both waveguide antennas consist of the same waveguides with radiating slots designed by traveling-wave excitation. The number of the radiating waveguide and the structures of the feeding circuits are different in the two antennas. Traveling-wave excitation is common technique in the designs of the slotted waveguide array antennas and the microstrip comb-line antenna. Array fed by

traveling-wave excitation suffer beam shift from frequency deviation, which causes narrow frequency bandwidth. However, in the case of narrow band application, traveling-wave excitation is quite effective to achieve high antenna efficiency.

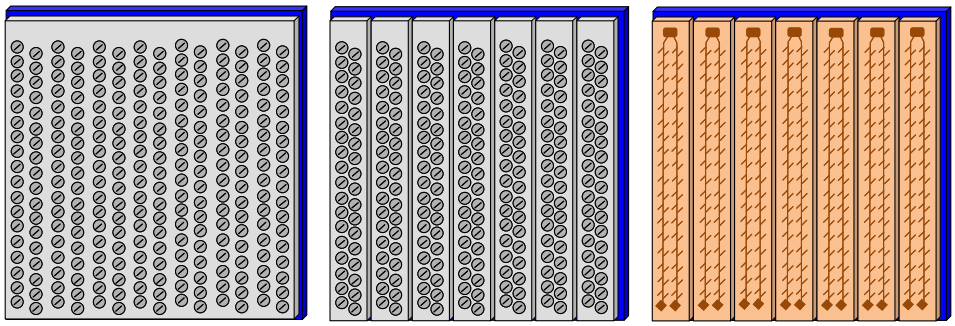

(a) Two-dimensional waveguide planar antenna

(b) Waveguide planar antenna composed of sub-arrays

(c) Microstrip comb-line antenna composed of sub-arrays

Fig. 1. Configurations of three planar antennas

2. Antenna configurations

Three different planar antennas are developed in the millimeter-wave band. Configurations of the antenna systems are shown in Fig. 1. Figure 1(a) shows a high-gain slotted waveguide antenna which has only one feeding port. Feeding network is included in the antenna. Second one in Fig. 1(b) is also a slotted waveguide antenna. However, the antenna system consists of some sub-arrays, each one of which has its own feeding port. Feeding network could be DBF systems or RF power divider with phase shifters for beam scanning. The waveguide antennas can be replaced by microstrip comb-line antenna for sub-arrays as shown in Fig. 1(c).

2.1 Slotted waveguide array antenna

We developed a design technology of slotted waveguide array antennas for arbitrarily linear polarization without growing grating lobes of two-dimensional array. Here, we designed an antenna with 45-degrees diagonal polarization to apply to automotive radar systems. Novel ideas to suppress grating lobes are supplied in the proposed structure of the two slot antennas in Fig. 1(a) and (b), which is still simple in order to reduce production cost. The configurations of the proposed antennas are shown in Fig. 2(a) and (b). All the radiating slots are cut at the center of the narrow wall of the radiating waveguides and are inclined by identically 45 degrees from the guide axis (x-axis) for the polarization requirement. The slotted waveguide planar antenna is composed of one feeding waveguide and two or 24 radiating waveguides. Spacing of slots in x-direction is one guided wavelength of the radiating waveguide. It is larger than a wavelength in free space. Grating lobes appear in zx-plane for one-dimensional array. Therefore, the radiating waveguides are fed in alternating 180 degrees out of phase since adjacent waveguides are spaced in a half guided wavelength $1/2\ \lambda_{gf}$ of the feeding waveguide. Slots are arranged with a half guided wavelength shift alternately in x-direction on each waveguide in order to compensate the phase difference

between the adjacent waveguides. Consequently, the grating lobes do not appear in *zx*-plane because the slot spacing becomes about a half guided wavelength in *x*-direction. However, the grating lobes still appear in the plane including *z*-axis and diagonal *kk'*-direction due to the triangular lattice arrangement since the slot spacing in *kk'*-direction becomes the maximum as is shown in Fig. 2(a). In order to suppress the grating lobes, we propose the post-loaded waveguide-slot with open-ended cavity shown in Fig. 3.

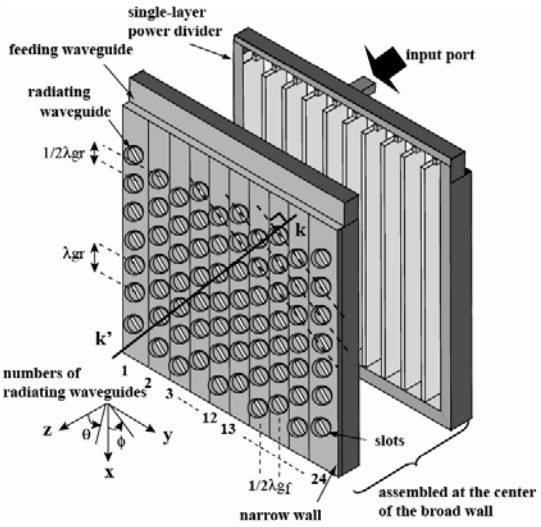

(a) Waveguide antenna with 24 radiating waveguides

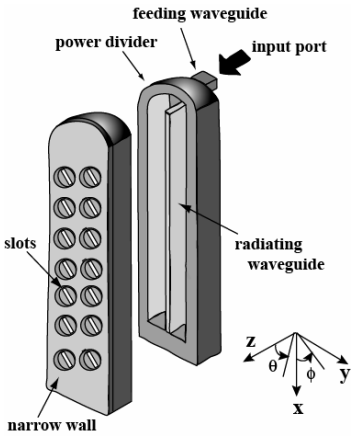

(b) Waveguide antenna with two radiating waveguides

Fig. 2. Configuration of slotted waveguide planar antennas

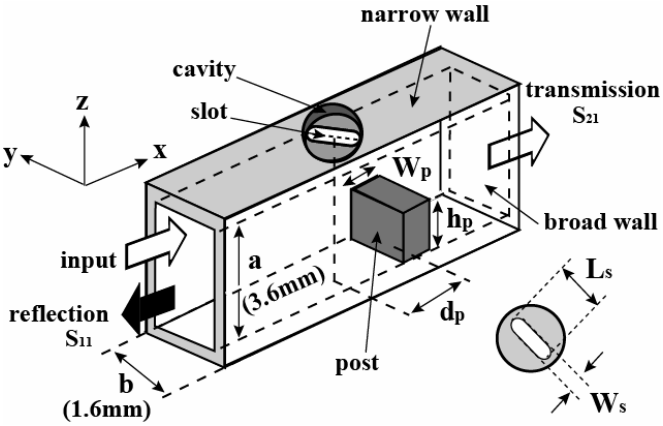

Fig. 3. Configuration of a post-loaded waveguide slot with open-ended cavity

A slot is cut on the narrow wall of the radiating waveguide. The spacing of radiating waveguides in *y*-direction can be short because the narrow-wall width is much smaller than the broad-wall width which is designed as a large value to reduce guided wavelength and

slot spacing in x-direction. Broad-wall width can be designed independently from slot spacing in y-direction. Slot length is designed for required radiation. Resonant slot is not used in this design. Radiation is not enough because slot length is limited by narrow-wall width. Furthermore, since broad-wall width is designed to be large in order to reduce guided wavelength, power density is small around the slot. So, in order to increase radiation, we propose to locate a post on the opposite side of the slot at the bottom of the radiating waveguide as is shown in Fig. 3. In the case that post is located in the waveguide, as the size of the cross section of the waveguide is small above the post, power density increases around the slot. Thus, radiation from the slot increases depending on the height of the post.

In order to improve the return loss characteristic of the array, previously mentioned conventional slotted waveguide arrays are often designed to have some degrees beam-tilting. However, in this case, it becomes the cause to generate grating lobes or to enhance their levels because the visible region of array factor changes. In terms of the proposed antenna, the post in the waveguide is designed to cancel the reflections from the slot and from the post by optimization of their spacing. Therefore, it is not necessary to use the beam-tilting technique because the reflection from each element has already been small due to the effect of the post. Furthermore, we set an open ended cavity around each slot. Since the cavity shades the radiation toward the low elevation angle, the grating lobe level is reduced effectively. Thus, we can suppress the grating lobes in the diagonal direction.

The proposed structure has a following additional advantage for low loss. The antenna is assembled from two parts, upper and lower plates to compose a waveguide structure. Since radiating slots are cut on the narrow wall of the waveguides, cut plane of the waveguide is xy-plane at the center of the broad wall, where the current flowing toward z-direction is almost zero. Therefore, transmission loss of the waveguide could be small. High efficiency is expected even without close contact between the two parts of the waveguide. The electric current distribution would be perturbed by existence of slots. However, since the current in z–direction is still small at the cut plane, it is expected that the proposed antenna structure is effective to reduce transmission loss in the antenna feed.

2.2 Microstrip comb-line antenna

A microstrip comb-line antenna is composed of several rectangular radiating elements that are directly attached to a straight feeding line printed on a dielectric substrate (Teflon-compatible Fluorocarbon resin film, thickness t = 0.127 mm, relative dielectric constant ε_r = 2.2 and loss tangent tan δ = 0.001) with a backed ground plane, as shown in Fig. 4. The width of the feeding microstrip line is 0.30 mm. The characteristic impedance of this line is 60 Ω. The radiating elements are inclined 45 degrees from the feeding microstrip line for the polarization requirement of automotive radar systems. The radiating elements with length L_{en} and width W_{en} are arranged on the both sides of the feeding line, which forms an interleaved arrangement in a one-dimensional array. The resonant length L_{en} is identical to a half guided wavelength. Element spacing d_{en} is approximately a half guided wavelength so that all the elements on the both sides of the microstrip line are excited in phase. A matching element is designed to radiate in phase all the residual power at the termination of the feeding line. Coupling power of radiating element is controlled by width W_{en} of the radiating element. Wide element radiates large power.

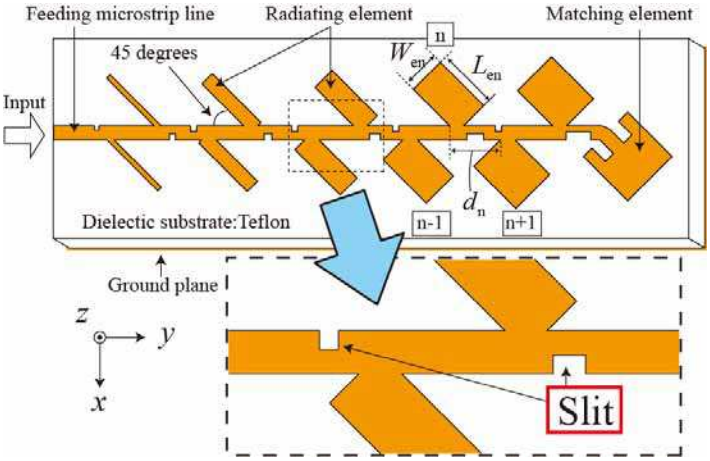

Fig. 4. Configuration of microstrip comb-line antenna with reflection-canceling slit structure

A radiation pattern with broadside beam is often used in many applications. However, when all the radiating elements are designed to excite in phase, all the reflections are also in phase at the feeding point, thus significantly degrading the overall reflection characteristic of the array. In the conventional design with beam tilting by a few degrees, reflections are canceled at the feed point due to the distributed reflection phases of the radiating elements. This means that the design flexibility of beam direction is limited by the reflection characteristics.

To solve this problem, we propose a reflection-canceling slit structure as shown in Fig. 4. A rectangular slit is cut on the feeding line near the radiating element. A reflection from each radiating element is canceled with the reflection from the slit. As the reflection from a pair of radiating element and slit is suppressed in each element, a zero-degree broadside array can be designed without increasing the return loss of the array. Because the sizes of all the radiating elements are different for the required aperture distribution, the slit dimensions and spacing of slit from the radiating element are optimized for each radiating element. Simple design procedure is required in the array design.

3. Design of linear array with traveling-wave excitation

Both waveguide antenna and microstrip antenna are designed in common procedure based on the traveling-wave excitation. Reflection wave is neglected in the design since reflection-canceling post and slit are used for the waveguide antenna and the comb-line antenna, respectively. Simple and straight-forward design procedure is expected in traveling-wave excitation. Here, design procedure based on traveling-wave excitation of the waveguide antenna is presented in this section.

A configuration of a post-loaded waveguide slot with open ended cavity is shown in Fig. 3. A slot element with post is designed at 76.5 GHz. The slot is cut on the waveguide narrow wall and is inclined by 45 degrees from the guide axis. The slot spacing becomes one guided wavelength which is larger than a wavelength in free space. The guided wavelength of the TE_{10} mode in the hollow waveguide is given by

$$\lambda_g = \frac{\lambda_0}{\sqrt{1-\left(\frac{\lambda_0}{2a}\right)^2}} \tag{1}$$

where λ_0 is a wavelength in free space and a is the broad-wall width of the waveguide. In order to become the guided wavelength short, the broad-wall width is determined to be large within the limit that only TE_{10} mode propagates. Broad-wall width is 3.92 mm in which cutoff frequency of TE_{10} mode is 76.5 GHz. The width is designed to be 3.6 mm taking production error and required frequency bandwidth into account. The guided wavelength of the radiating waveguide (3.6 mm X 1.6 mm) is 4.67 mm which is shorter than 5.06 mm of standard waveguide (3.1 mm X 1.55 mm). Slot spacing in x-direction can be short by increasing the broad-wall width a of the waveguide. The spacing in y–direction is about 2.6 mm because the wall thickness is about 1.0 mm. Consequently, the spacing in kk'-direction becomes about 3.48 mm ($0.89\,\lambda_0$) and the grating lobe would be suppressed.

Radiation is controlled by both the slot length L_s and the post height h_p. The slot width W_s is 0.4 mm. Edge of slot forms semicircle of radius 0.2 mm for ease in manufacturing. Narrow-wall width b of waveguide is determined as 1.6 mm to cut the 45-degrees inclined slot of maximum slot length 2.0 mm. The post width W_p is 0.5 mm. Each slot element with post is designed to obtain the desired radiation and reflection lower than –30 dB at the design frequency. The reflection characteristic is controlled by changing the post height h_p and the post offset d_p from the center of the slot for several slot lengths. They are calculated by using the electromagnetic simulator of finite element method. Coupling C is defined as radiating from the waveguide to the air through the slot and is given by

$$C = \{1 - |S_{11}|^2 - |S_{21}|^2\} \times 100\ [\%] \tag{2}$$

where S_{11} is reflection and S_{21} is transmission of the waveguide with slot in the analysis model shown in Fig. 3. Figure 5 shows simulated frequency dependency of reflection S_{11}, transmission S_{21} and coupling C in the case of maximum slot length 2.0 mm. The coupling was approximately 56.9%, where h_p and d_p are 1.6 and 0.6 mm, respectively. It is more than three times as large as coupling 18% from the slot without post. It is confirmed that large coupling is achieved due to the post even though the broad-wall width is large. Figure 6 shows the slot length L_s, the post height h_p and the post offset d_p from the center of the slot depending on coupling. Large slot length L_s is required for large coupling. In order to cancel the reflections from slot and post, amplitude of the reflections should be equal and phase difference should be 180 degrees out of phase. The post height h_p is also large for large coupling to satisfy the amplitude condition. The post offset d_p from the center of the slot gradually increases for the phase condition because perturbation of reflection phase grows for increasing slot length.

An open ended cavity is set on each slot. Since the cavity shades the radiation from the slots to the low elevation angle, the grating lobe level is reduced. Figure 7 shows calculated element radiation pattern and array factors in kk'-z plane. Element radiation pattern without cavity is ideally identical to isotropic radiation pattern because it is the radiation pattern of slot element in the perpendicular plane to the slot axis (E-plane). Difference of the levels in the element radiation patterns with and without cavity is approximately 14 dB at 90 degrees from broadside direction. Sidelobes of total radiation pattern are suppressed in large angle

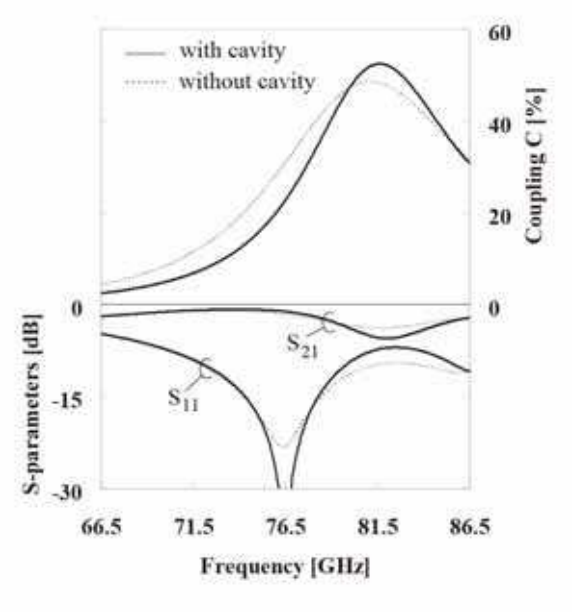

Fig. 5. Simulated frequency dependency of S_{11}, S_{21} and coupling C

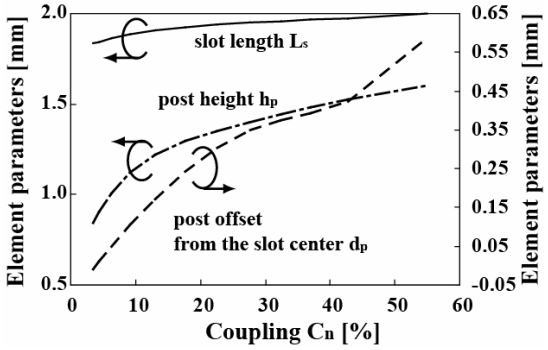

Fig. 6. Slot length, post height and offset from the center of the slot versus coupling

from the broadside. It is observed that the grating lobe level of antenna without cavities is –22 dB, which is suppressed to –36 dB by using cavity. However, radiation pattern near broadside is almost the same and independent on the cavity. No mutual coupling between slots are taken into account in the design because the mutual coupling is very small due to the element radiation pattern of cavity. Simple design procedure can be applied. The effect of the circular cavity to the slot impedance and coupling is shown in Fig. 5. High-Q resonance characteristic of cavity structure is observed, that is, maximum coupling power is larger when cavity is installed, on the other hand, coupling power from slot with cavity is smaller than without cavity in lower frequency than resonance. Since optimum parameters for minimum S_{11} are slightly different between with and without cavity, level of S_{11} without cavity does not fall down at the design frequency.

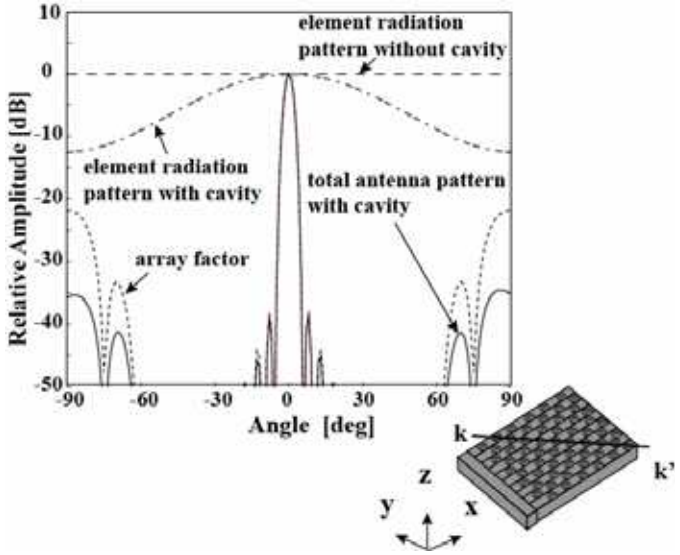

Fig. 7. Element radiation pattern of slot with cylindrical cavity and total radiation pattern which is product of array factor and element radiation pattern of slot with cylindrical cavity in diagonal plane (*kk'*-*z* plane)

A 13-element array is designed at 76.5 GHz. Thirteen radiating slots are arranged on one radiating waveguide, which corresponds to a linear array antenna. A terminated element composed of a post-loaded slot and a short circuit is used at the termination of each radiating waveguide. All the remaining power at the termination radiates from the element and also contributes antenna performance. Reflections from all the elements are suppressed by the function of post-loaded slot. So, design procedure for traveling-wave excitation is implemented (Sakakibara, 1994). Thirteen slot elements are arrayed and numbered from the feed point to the termination. Required coupling from slots are assigned for Taylor distribution on the aperture to be a sidelobe level lower than –20 dB. Incidence $P_w(n)$, transmission $P_w(n+1)$ and radiation $P_r(n)$ of nth slot shown in Fig. 8 are related by

$$P_w\,(n+1) = P_w(n) - P_r(n) \tag{3}$$

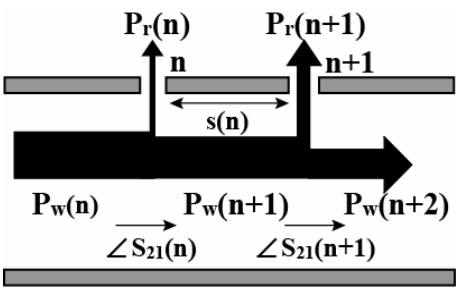

Fig. 8. Relation of radiation and transmission versus input. Slot spacing is related to transmission phase.

Coupling C_n is defined by

$$C_n = \frac{P_r(n)}{P_W(n)} \times 100(\%) \qquad (n = 1,2,3,\cdots,12) \tag{4}$$

The previously mentioned parameters L_s, h_p and d_p are optimized in each slot element shown in Fig. 9. A required variety of coupling is 3.5% ~ 54.9%. Element spacings $s(n)$ are determined to realize uniform phase distribution. This condition imposes

$$k_g s(n) = 2\pi + \angle S_{21}(n) \tag{5}$$

$$s(n) = \lambda_g + \frac{\angle S_{21}(n)}{2\pi} \lambda_g \tag{6}$$

where k_g (= $2\pi/\lambda_g$) is the wave number of the waveguide and $\angle S_{21}(n)$ is phase advance perturbed by the slot element as is shown in Fig. 8. As $\angle S_{21}(n)$ is positive value, element spacing becomes slightly larger than a guided wavelength. This phase perturbation is simulated accurately by using electromagnetic simulator. So, the above design procedure dispenses with iteration.

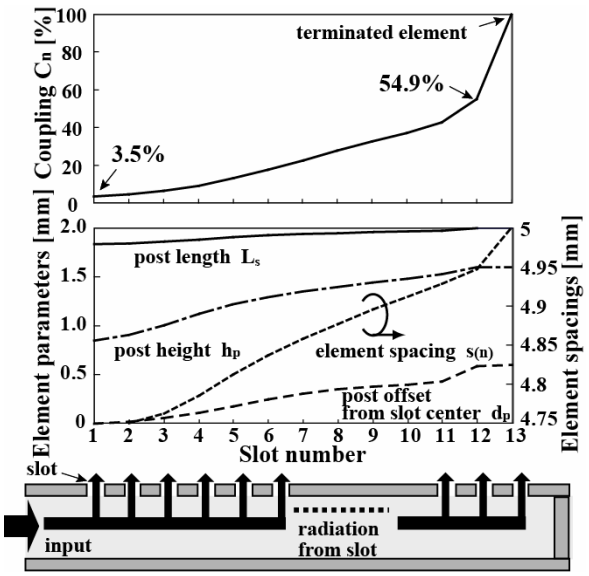

Fig. 9. Assigned coupling and dimensions of array elements for Taylor distribution on the aperture to be a sidelobe level lower than –20 dB.

4. Design of feeding circuits

The developed linear arrays are arranged to compose two-dimensional planar array. Required feeding circuits depend on the transmission lines and the number of the linear

arrays. Waveguide 24-way and two-way power dividers are developed to feed the waveguide antennas. Microstrip-to-waveguide transition is also developed to feed the microstrip comb-line antenna from waveguide.

4.1 Waveguide feeding 24-way power divider

In the development of the two-dimensional planar waveguide antennas, a single-layer 24-way power divider composed of E-plane T-junctions feeding narrow-wall slotted waveguide planar array are designed as is shown in Fig. 2(a). It is composed of one feeding waveguide and 24 radiating waveguides slotted on the narrow walls. The antenna input port is located at the center of the feeding waveguide. All the radiating waveguides are fed from the feeding waveguide. The radiating waveguides are connected on the broad wall of the feeding waveguide, which forms a series of E-plane T-junctions shown in Fig. 10(a) (Mizutani et al. 2005). The broad-wall width of the feeding waveguide is determined so that the guided wavelength of feeding waveguide corresponds just twice the narrow-wall width of the radiating waveguide including the wall thickness between the radiating waveguides since adjacent waveguides are fed in an alternating 180 degrees out of phase. A coupling window is opened at each junction. Coupling to the radiating waveguide is controlled by the window width W_f in the H-plane. A post is set at the opposite side of the coupling window to obtain large coupling into the radiating waveguide and to cancel the reflections from the window and the post out of phase. Reflection level and phase of the post are adjusted to cancel both reflections by changing the post length L_f and the post offset d_f from the center of the window, respectively. Two edge radiating waveguides are fed from

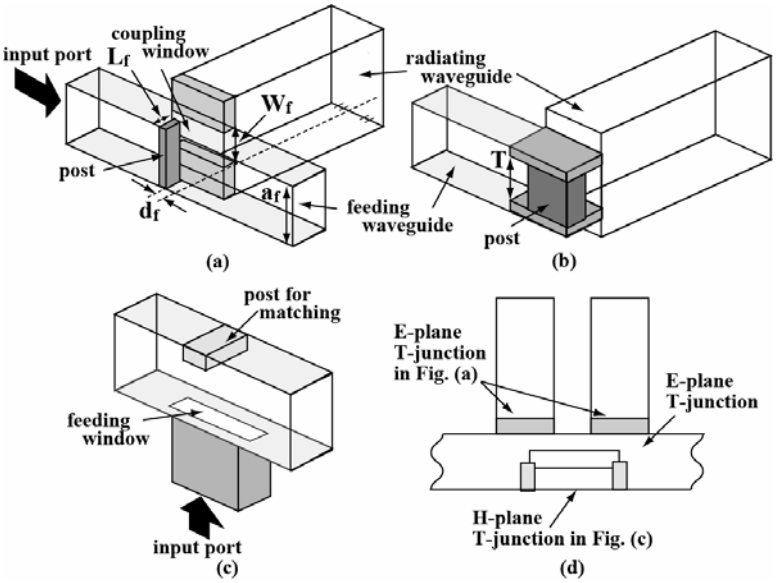

Fig. 10. Configuration of several parts of feeding circuit. (a) T-junction. (b) Terminated E-bend. (c) H-plane T-junction for input. (d) Top view and analysis model of the input H-plane T-junction on bottom plate around the antenna feed port with adjacent radiating waveguide.

terminated E-bends, shown in Fig. 10(b), in order to make all the remaining power contribute to the antenna performance. The size of the post is designed for matching and the width T of the waveguide is a parameter for phase adjustment of wave into the radiating waveguide. The feeding waveguide is fed through the H-plane T-junction at the input port shown in Fig. 10(c). Since the two adjacent radiating waveguides are very close to the input port, the H-plane T-junction is designed taking the effect of the two radiating waveguides into consideration as the analysis model is shown in Fig. 10(d). Phase perturbation of each E-plane T-junction is evaluated by electromagnetic simulator. The phase delay is compensated by adjustment of the spacing between radiating waveguides.

In order to feed radiating waveguides in alternating 180 degrees out of phase, we designed the E-plane T-junctions. The broad-wall width a_f of the feeding waveguide is designed to be 2.45 mm. So, the guided wavelength of the feeding waveguide is 6.6 mm calculated by equation (1). Required coupling to each radiating waveguide is assigned for Taylor distribution on the aperture as is shown in Fig. 11 to be a sidelobe level lower than –20 dB as well as the design of slotted linear array mentioned in the previous section. Geometrical parameters of each junction are also shown in this figure. Input port is at the center of the feeding waveguide and aperture distribution is designed to be symmetrical. So, only one half from port 13 to 24 is shown here. A required variety of coupling is 13.8% ~ 51.6%. The previously mentioned parameters L_f, W_f and d_f are optimized for each T-junction by using the electromagnetic simulator of finite element method. The window width W_f gradually increase with port number because required coupling increases. Relatively large windows are used at the center of the port numbers 12 and 13 to compensate the effect of the mutual coupling from the closely-located input port. The post length L_f also increases with port number to cancel the reflection from the window because the reflection coefficient of the large window is large. Furthermore, the post offset d_f from the center of the window gradually increases for the phase condition to cancel reflections because perturbation of reflection phase grows for increasing window width W_f and post length L_f.

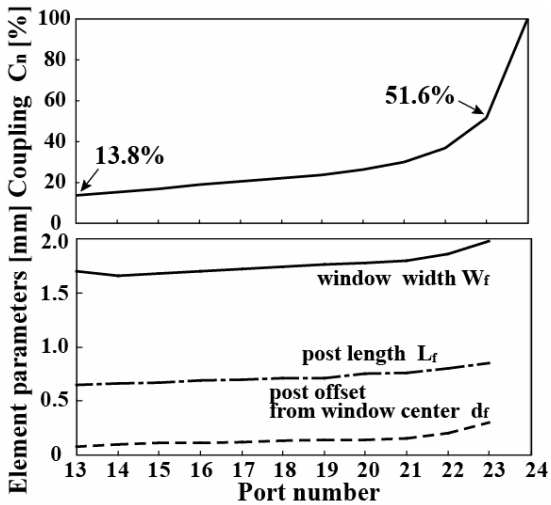

Fig. 11. Coupling of T-junctions for Taylor distribution and geometrical parameters of T-junction to be a sidelobe level lower than –20 dB.

A 24-way power divider is designed at 76.5 GHz. Field amplitude and phase distributions of the twenty four output ports are shown in Fig. 12. The simulated and measured results almost agree well with the design having the error smaller than 1 dB in amplitude and 5 degrees in phase. Simulated frequency dependency of reflection of the input T-junction with and without all the twenty four input ports is shown in Fig. 13. Resonant frequency is observed at the design frequency 76.5 GHz. Bandwidth of the reflection below –20 dB is approximately 8 GHz.

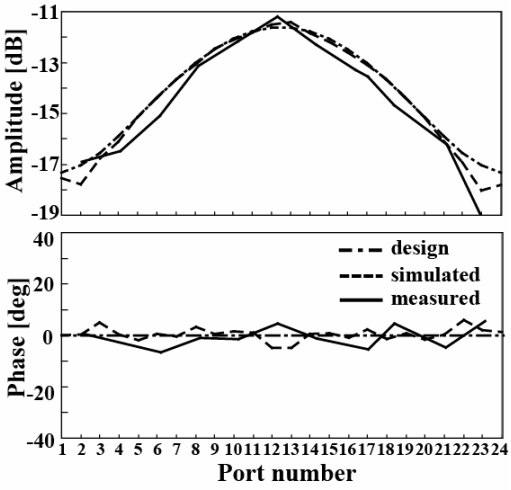

Fig. 12. Output amplitude and phase distributions of the single layer power divider

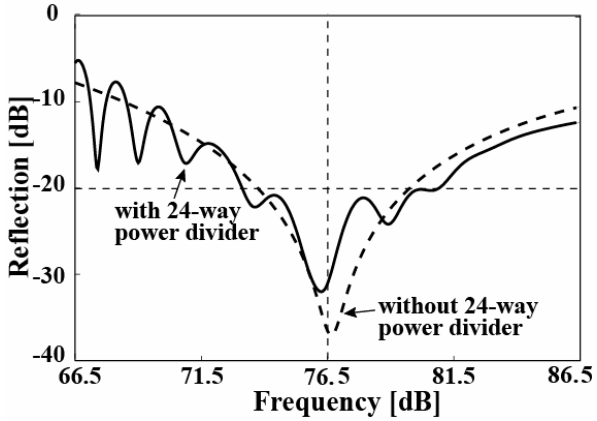

Fig. 13. Simulated frequency dependency of reflection of the input T-junction with and without 24-way power divider

4.2 Waveguide feeding two-way power divider

In order to excite all the slots in phase with a triangular lattice arrangement in the two-waveguide antenna, two radiating waveguides are fed in 180 degrees out of phase each

other. We propose the compact power divider for the feeding circuit of the sub-array as shown in Fig. 14. The feeding waveguide is connected at the junction of the two radiating waveguides from the opposite side of the slots. There is a feeding window at the boundary between the radiating waveguide and the feeding waveguide for matching. A matching post is installed at the opposite side of the feeding window. The reflection characteristic is controlled by changing the size of the feeding window W_a, W_b and the height h_p of the matching post. The size of the feeding waveguide is W_{a0}, W_{b0} (3.10 X 1.55 mm) and the broad wall width of the radiating waveguide is h_{p0} (3.6mm). Figures 15(a), (b) and (c) shows the reflection characteristic depending on the height of the matching post h_p, the broad width W_a and the narrow width W_b of the feeding waveguide, respectively. Minimum reflection is obtained when the height h_p of the matching post is 0.40 h_{p0} and the broad width W_a and narrow width W_b of the feeding window are 1.0 W_{a0} and 0.65 W_{b0}, respectively.

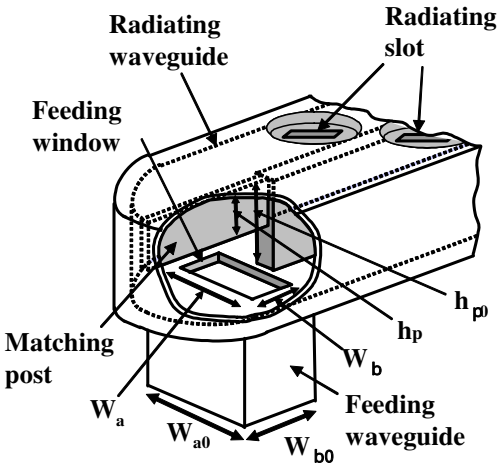

Fig. 14. Configuration of waveguide two-way power divider.

4.3 Design of microstrip-to-waveguide transition for feeding microstrip antenna

For feeding circuit of microstrip comb-line antenna from waveguide, microstrip-to-waveguide transition is developed. Ordinary microstrip-to-waveguide transitions require back-short waveguide on the substrate. In order to reduce number of parts and assembling error of the back-short waveguide, transition with planar structure is developed (Iizuka et al. 2002). Figure 16 shows a configuration of the planar microstrip-to-waveguide transition. A microstrip substrate with metal pattern is on the open-ended waveguide. Microstrip line is inserted into the ground pattern of waveguide short on the upper plane of the substrate. Electric current on the microstrip line is electromagnetically coupled to the current on the patch in the aperture at the lower plane of the substrate. Via holes surround the waveguide in the substrate to prevent leakage. Figure 17 shows S_{11} and S_{21}. Resonant frequency of S_{11} is observed at the design frequency 76.5 GHz. Insertion loss of the transition is approximately 0.3 dB at 76.5 GHz.

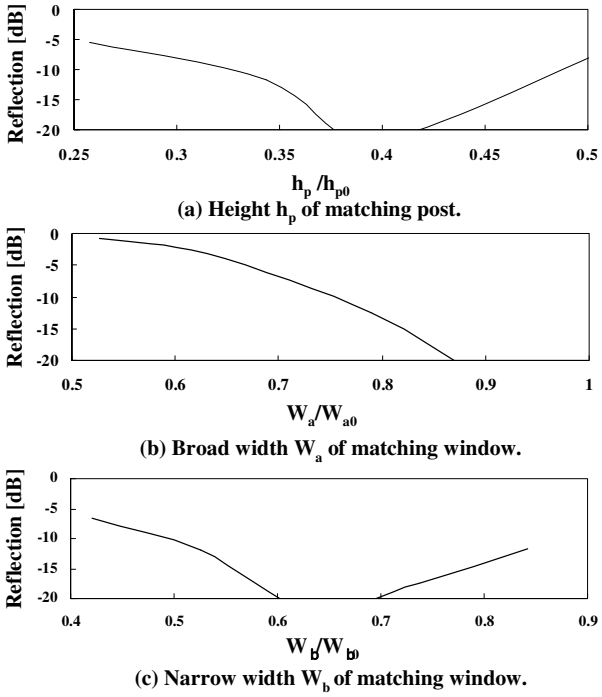

Fig. 15. Reflection characteristics of the waveguide two-way power divider

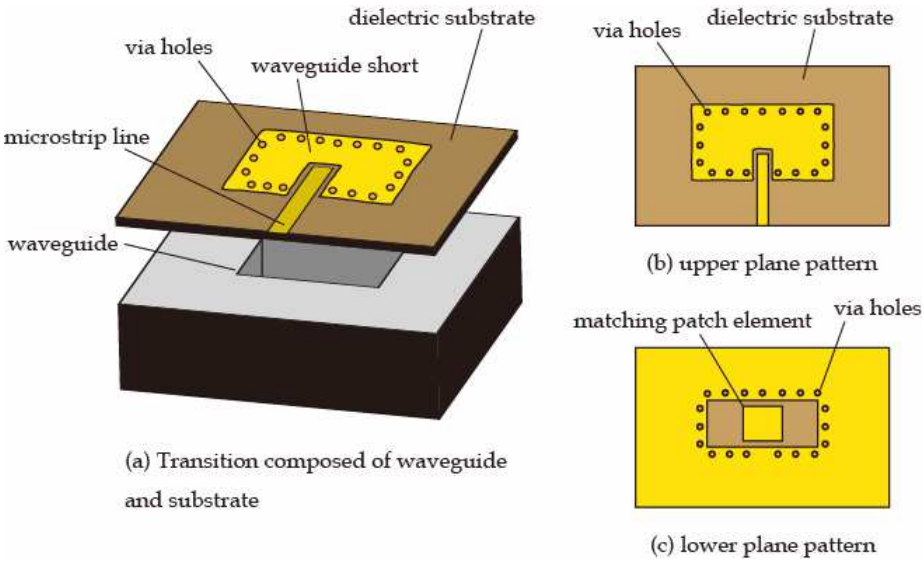

Fig. 16. Microstrip-to-waveguide transition with planar structure

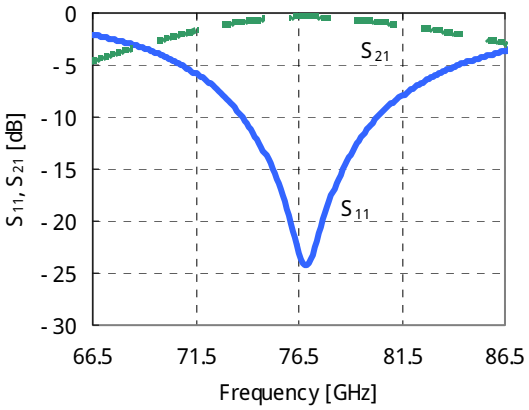

Fig. 17. Simulated S-parameters of the transition

5. Experiments

5.1 24-waveguide antenna

A 24-waveguide planar antenna is fabricated to evaluate the antenna performance. The photograph of the antenna is shown in Fig. 18. The fabricated antenna is assembled from two parts, upper and bottom aluminum plates with groove structures to compose waveguides. Cut plane is at the center of the broad wall of the waveguide and are fixed by screws. Twenty-four waveguides with 13 slots are arranged in parallel. Consequently, aperture size of antenna is 71.5 mm (in *x*-direction) × 64.7 mm (in *y*-direction).

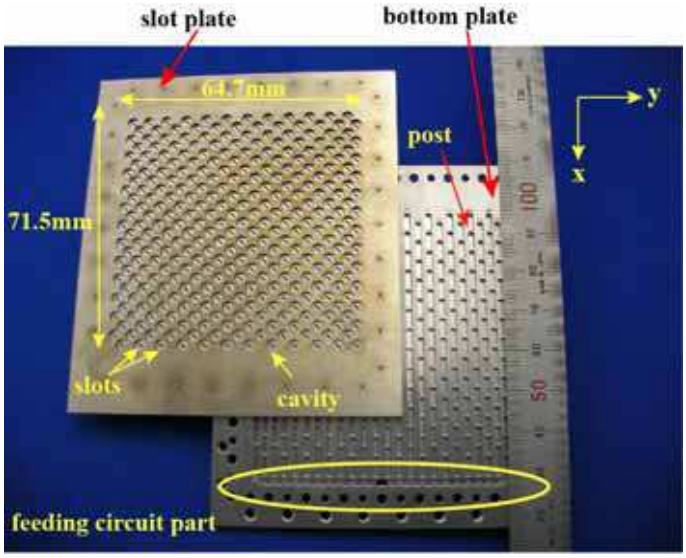

Fig. 18. Photograph of the fabricated antenna composed of the two plates

We discuss performance of the fabricated planar antenna in this section. Figure 19(a) shows the measured and designed radiation patterns in *zx*-plane at 76.5 GHz. The measured main beam direction results in –0.5 degrees from *z*-axis. This beam squint is due to error in the estimation of phase perturbation for transmission through the radiating elements of slots.

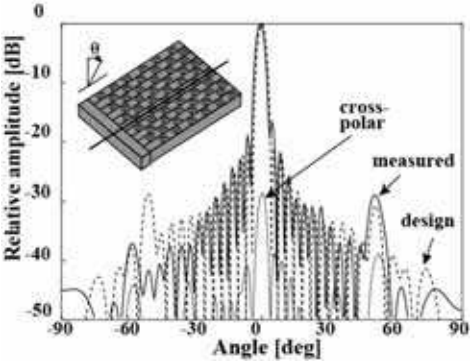

Fig. 19(a) Radiation patterns in *zx*-plane

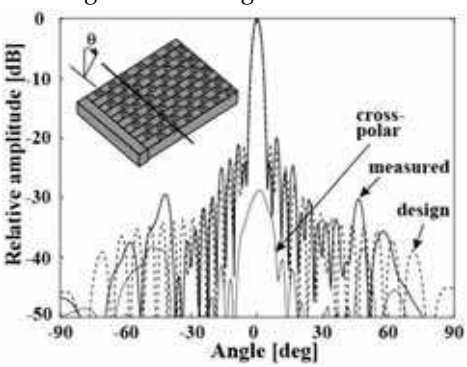

Fig. 19(b) Radiation patterns in *yz*-plane

The sidelobe level is –16.8 dB which is 3.2 dB higher than design. Figure 19(b) shows radiation patterns in *yz*-plane. The main beam directs to the broadside as the same with design. Measured sidelobe level is –20.0 dB, which also almost agrees well with the design. Measured cross-polar patterns are also shown in Figs. 19(a) and (b). XPD (cross polarization discrimination) is 28.7 dB. Figure 20 shows the measured two-dimensional radiation patterns. In contrast to the general slotted waveguide arrays, maximum grating lobe level of the proposed antenna is suppressed to –28.6 dB. Figure 21 shows the measured gain and antenna efficiency at the frequency from 74 to 78 GHz. The center frequency shifts in 500 MHz from the design frequency 76.5 to 76.0 GHz. The gain is 33.2 dBi and the antenna efficiency is 56% at 76.0 GHz. Total loss 44% is estimated to consist of mismatch 3%, directivity of Taylor distribution 1% and cross-polarization 1%. Rest of them 39% is considered to be a feeding loss due to the imperfect waveguide in the millimeter-wave band. Bandwidth of gain over 30 dBi is approximately 1.9 GHz. High gain and high antenna

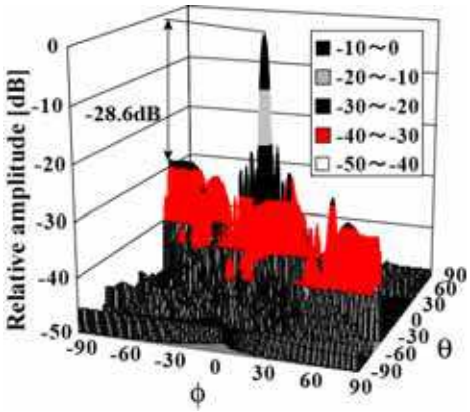

Fig. 20. Two-dimensional radiation pattern

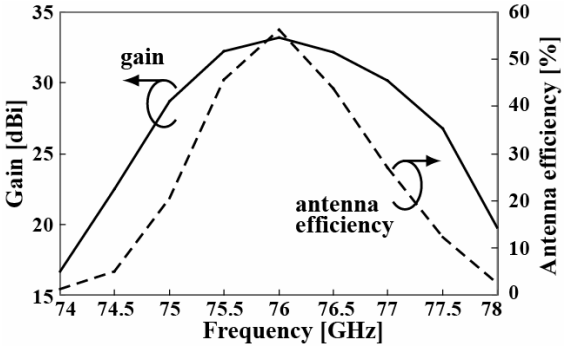

Fig. 21. Measured gain and antenna efficiency

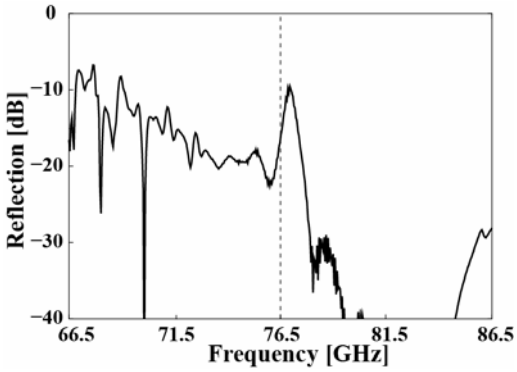

Fig. 22. Measured frequency dependency of reflection at the input port

efficiency are achieved. The measured reflection characteristics are indicated in Fig. 22. The measured reflection level is –22.0 and –16.5 dB at 76.0 and 76.5 GHz, respectively. On the other hand, large reflection is observed at 77.0 GHz, whose level is –10 dB. It is one of the causes of gain degradation. The cause of reflection increasing at 77.0 GHz would be that the proposed slot element is narrow frequency band width as is shown in Fig. 5. All the reflections from antenna elements due to frequency shift of fabrication error would be summed up in phase at 77.0 GHz.

5.2 Two-line waveguide antenna

The designed antenna was fabricated and feasibility was confirmed by experiments. Photograph of the developed antenna is shown in Fig. 23. Two metal plates of aluminium alloy were screwed together. Cut plane is at the center of the waveguide broad wall as well as the 24-waveguide antenna shown in the previous section. Posts were located in the waveguide to increase radiation from slots and to improve reflection characteristics. The cavity was set on each slot.

Figure 24(a) shows measured and simulated radiation patterns in the plane parallel to the waveguide axis at the design frequency 76.5 GHz. Beam direction was approximately 0 degree as was the same with the broadside beam design. Sidelobe level was around –20 dB as was almost the same level with the design of Taylor distribution for –20 dB sidelobe level.

Fig. 23. Photograph of the two-line waveguide antenna

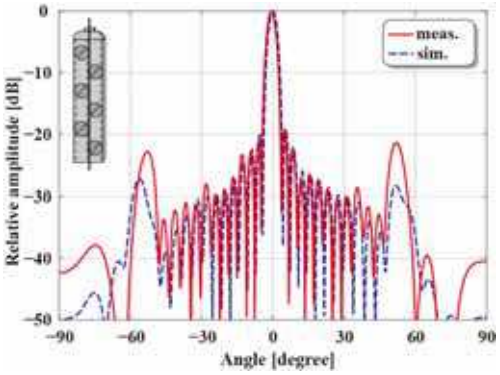

Fig. 24(a) Radiation pattern in the plane parallel to the waveguide

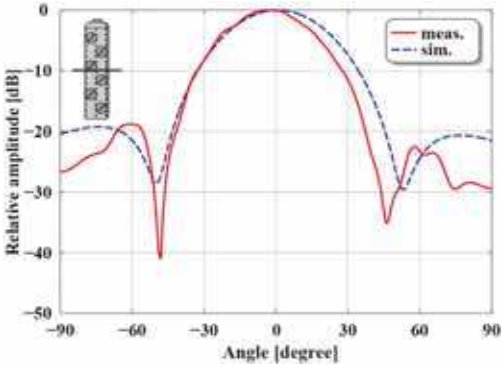

Fig. 24(b) Radiation patterns in the plane perpendicular to the waveguide

Some portion of the grating lobes were observed in 50 degrees which were about 7 dB higher than the simulation and still lower than –20 dB. Figure 24(b) shows measured and simulated radiation patterns at 76.5 GHz in the plane perpendicular to the waveguide. Almost symmetrical radiation pattern was obtained in the experiment. Sidelobe level was around –20 dB as was the same with the simulation. Figure 25 shows reflection

characteristics. Since the resonant frequency corresponded to the design frequency 76.5 GHz, reflection level was lower than −20 dB at the frequency. Although the bandwidth was wider than 3 GHz for reflection lower than −10 dB, the center frequency of the bandwidth shifted by a few GHz lower than the design frequency. Figure 26 shows gain and antenna efficiency. Gain and antenna efficiency were 21.1 dBi and 51 %, respectively. They were degraded in the lower frequency band due to the return loss mentioned in Fig. 25. However, the efficiency was still relatively high compared with other millimeter-wave planar antennas.

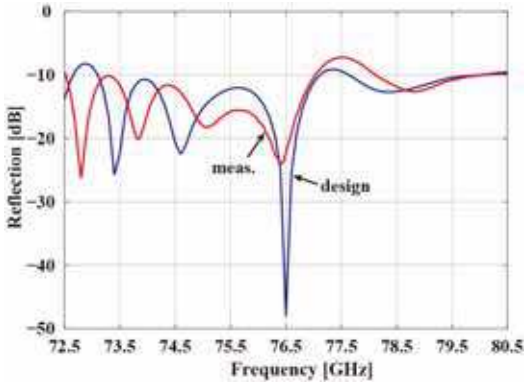

Fig. 25. Reflection characteristics

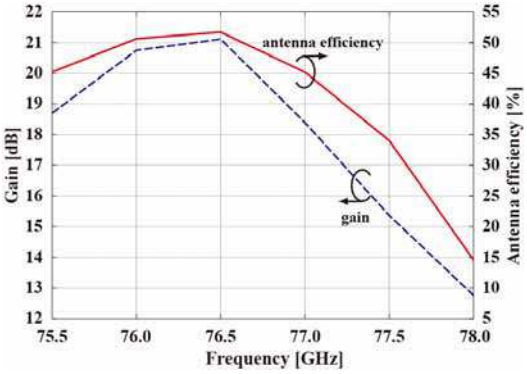

Fig. 26. Gain and antenna efficiency

5.3 Microstrip comb-line antenna

Microstrip comb-line antenna with two lines of 27 elements and with broadside beam is fabricated for experiments as is shown in Fig. 27. Reflection level of the fabricated antenna is −12.9dB at the design frequency 76.5 GHz as shown in Fig. 28. Measured beam direction in the plane parallel to the feeding line is −1.0 degree, and sidelobe level is −17.9 dB shown in Fig. 29(a). Symmetrical radiation pattern is obtained in the plane perpendicular to the feeding line as shown in Fig. 29(b). The measured radiation pattern almost agrees well with the array factor. High antenna efficiency 55 % with antenna gain 20.3 dBi is obtained at the design frequency 76.5 GHz. The efficiency is almost the same level with the two-waveguide antenna.

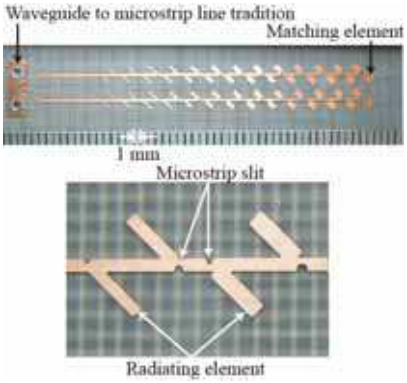

Fig. 27. Photographs of the developed microstrip comb-line antenna

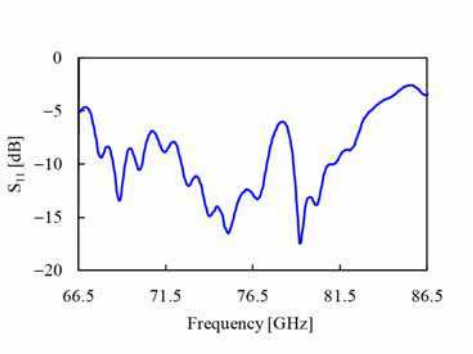

Fig. 28. Measured reflection characteristics

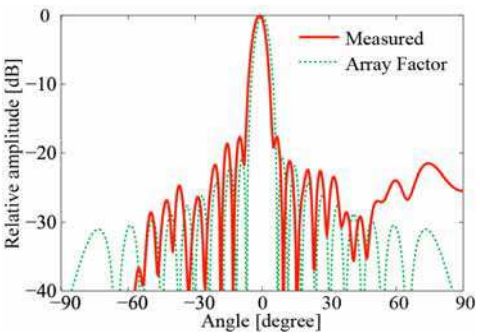

Fig. 29(a) Radiation pattern in the plane parallel to the feeding line

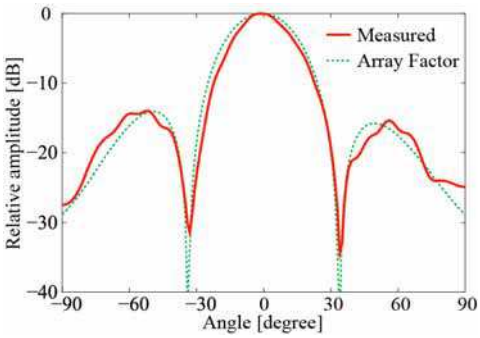

Fig. 29(b) Radiation pattern in the plane perpendicular to the feeding line

6. Conclusion

We have developed three types of millimeter-wave low-profile planar antennas; high-gain two-dimensional planar waveguide array antenna with 24 waveguides, two-line waveguide antenna and microstrip comb-line antenna which can be applied to the sub-arrays for beam-scanning antennas. Microstrip comb-line antenna is advantageous at the points of low cost and lower feeding loss compared with other microstrip array antennas. High efficiency is achieved, which is almost the same level with the waveguide when the aperture size and gain is relatively small. Waveguide antenna possesses much higher performance capability due to the low loss characteristic of waveguide feeding when the aperture size and gain is large. However, cost reduction is one of the most serious problems for mass production. Metal injection molding could be a solution for the waveguide antenna.

7. References

Asano, Y. (2000). Millimeter-wave Holographic Radar for Automotive Applications, *2000 Microwave workshops and exhibition digest, MWE 2000*, pp. 157-162, Yokohama, Japan, Dec. 2000

Fujimura, K. (1995). Current Status and Trend of Millimeter-Wave Automotive Radar, *1995 Microwave workshops and exhibition digest, MWE'95*, pp. 225-230, Yokohama, Japan, Dec. 1995

Hayashi, Y.; Sakakibara, K.; Kikuma, N. & Hirayama, H., (2008). Beam-Tilting Design of Microstrip Comb-Line Antenna Array in Perpendicular Plane of Feeding Line for Three-Beam Switching, *Proc. 2008 IEEE AP-S International Symposium and USNC/URSI National Radio Science Meeting*, 108.5, ISBN 978-1-4244-2042-1, San Diego, CA, July 2008

Iizuka, H.; Watanabe, T.; Sato, K.; Nishikawa, K. (2002). Millimeter-Wave Microstrip Line to Waveguide Transition Fabricated on a Single Layer Dielectric Substrate," IEICE Trans. Commun., vol. E85-B, NO.6, June 2002, pp.1169-1177, ISSN 0916-8516

Iizuka, H.; Watanabe, T.; Sato, K. & Nishikawa, K. (2003). Millimeter-Wave Microstrip Array Antenna for Automotive Radars," *IEICE Trans. Commun.*, vol. E86-B, NO. 9, Sept. 2003, pp. 2728-2738, ISSN 0916-8516

Kitamori, N.; Nakamura, F.; Hiratsuka, T.; Sakamoto, K. & Ishikawa, Y. (2000). High-ε Ceramic Lens Antenna with Novel Beam Scanning Mechanism, *Proc. 2000 Int. Symp. Antennas and propagat., ISAP 2000*, vol. 3, pp.983-986, Fukuoka, Japan, Aug. 2000

Menzel, W.; Al-Tikriti, M. & Leberer, R. (2002). A 76 GHz Multiple-Beam Planar Reflector Antenna, *European Microw. Conf.*, pp. 977-980, Milano, Italy, Sept. 2002

Mizutani, A.; Yamamoto, Y.; Sakakibara, K.; Kikuma N. & Hirayama H., (2005). Design of Single-Layer Power Divider Composed of E-plane T-juctions Feeding Waveguide Antenna, *Proc. 2005 Int. Symp. Antennas and propagat., ISAP 2005*, vol. 3, pp. 925-928, Seoul, Korea, Aug. 2005.

Mizutani, A.; Sakakibara, K.; Kikuma, N. & Hirayama, H., (2007). Grating Lobe Suppression of Narrow-Wall Slotted Hollow Waveguide Millimeter-Wave Planar Antenna for Arbitrarily Linear Polarization, *IEEE Trans. Antennas and Propag.*, Vol. 55, No. 2, Feb. 2007

Park, S.; Okajima, Y.; Hirokawa, J. & Ando, M., (2005). A Slotted Post-Wall Waveguide Array With Interdigital Structure for 45◦ Linear and Dual Polarization, *IEEE Trans. Antennas Propag.*, vol. 53, no. 9, Sept. 2005, pp.2865-2871, ISSN 0018-926X

Sakakibara, K.; Hirokawa, J.; Ando, M. & Goto, N., (1994). A Linearly-Polarized Slotted Waveguide Array Using Reflection-Cancelling Slot Pairs," *IEICE Trans. Commun.*, vol. E77-B, NO. 4, Apr. 1994, pp. 511-518, ISSN 0916-8516

Sakakibara, K.; Hirokawa, J.; Ando, M. & Goto, N. (1996). Single-layer slotted waveguide arrays for millimeter wave application," *IEICE Trans. Commun.*,vol. E79-B, NO. 12, Dec. 1996, pp. 1765-1772, ISSN 0916-8516

Sakakibara, K.; Watanabe, T.; Sato, K.; Nishikawa, K. & Seo, K., (2001). Millimeter-Wave Slotted Waveguide Array Antenna Manufactured by Metal Injection Molding for Automotive Radar Systems, *IEICE Trans. Commun.*, vol. E84-B, NO. 9, Sept. 2001, pp. 2369-2376, ISSN 0916-8516

Sakakibara, K.; Kawasaki, A.; Kikuma, N. & Hirayama, H., (2008). Design of Millimeter-wave Slotted-waveguide Planar Antenna for Sub-array of Beam-scanning Antenna, Proc. 2008 Int. Symp. Antennas and Propagation, ISAP 2008, pp. 730-733, Taipei, Taiwan, Oct. 2008

Tokoro, S. (1996). Automotive Application Systems Using a Millimeter-wave Radar," *TOYOTA Technical Review*, vol.46 No.1, May 1996, pp. 50-55

Volakis, J. L. (2007). *Antenna Engineering Handbook*, Chap. 9, McGraw-Hill, ISBN 0-07-147574-5, New York

Yamamoto, Y.; Sakakibara, K.; Kikuma, N. & Hirayama, H., (2004). Grating Lobe Suppression of Narrow Wall Slotted Waveguide Array Antenna Using Post, *Proc. 2004 Int. Symp. Antennas and propagat., ISAP'04*, vol. 4, pp. 1233-1236, Sendai, Japan, Aug. 2004

Radar Technology

Edited by Guy Kouemou

ISBN 978-953-307-029-2
Hard cover, 410 pages
Publisher InTech
Published online 01, January, 2010
Published in print edition January, 2010

In this book “Radar Technology”, the chapters are divided into four main topic areas: Topic area 1: “Radar Systems” consists of chapters which treat whole radar systems, environment and target functional chain. Topic area 2: “Radar Applications” shows various applications of radar systems, including meteorological radars, ground penetrating radars and glaciology. Topic area 3: “Radar Functional Chain and Signal Processing” describes several aspects of the radar signal processing. From parameter extraction, target detection over tracking and classification technologies. Topic area 4: “Radar Subsystems and Components” consists of design technology of radar subsystem components like antenna design or waveform design.

How to reference

In order to correctly reference this scholarly work, feel free to copy and paste the following:

Kunio Sakakibara (2010). High-Gain Millimeter-Wave Planar Array Antennas with Traveling-Wave Excitation, Radar Technology, Guy Kouemou (Ed.), ISBN: 978-953-307-029-2, InTech, Available from: http://www.intechopen.com/books/radar-technology/high-gain-millimeter-wave-planar-array-antennas-with-traveling-wave-excitation

INTECH
open science | open minds

InTech Europe
University Campus STeP Ri
Slavka Krautzeka 83/A
51000 Rijeka, Croatia
Phone: +385 (51) 770 447
Fax: +385 (51) 686 166
www.intechopen.com

InTech China
Unit 405, Office Block, Hotel Equatorial Shanghai
No.65, Yan An Road (West), Shanghai, 200040, China
中国上海市延安西路65号上海国际贵都大饭店办公楼405单元
Phone: +86-21-62489820
Fax: +86-21-62489821